

# Colossal magnetoresistance in the antiferromagnetic $\text{La}_{0.5}\text{Ca}_{0.5}\text{MnO}_3$ system

G. Q. Gong, C. L. Canedy, and Gang Xiao<sup>a)</sup>  
*Physics Department, Brown University, Providence, Rhode Island 02912*

J. Z. Sun, A. Gupta, and W. J. Gallagher  
*IBM Research Division, Yorktown Heights, New York 10598*

We have explored the colossal magnetoresistance (CMR) effect in the antiferromagnetic  $\text{La}_{0.5}\text{Ca}_{0.5}\text{MnO}_3$  compound. In the absence of a magnetic field ( $H$ ), the solid is a canted antiferromagnetic (AFM) insulator. An applied  $H$  in the Tesla scale induces a first order AFM to FM phase transition, and correspondingly, an insulator to metal transition. The observed CMR is attributed to the  $H$ -induced charge localization-delocalization behavior associated with the AFM–FM transition. At low temperatures ( $T < 100$  K), the solid remains in the AFM phase, where we have observed a phenomenal one millionfold change in resistivity between 0 and 8 Tesla. The origin of CMR in low  $T$ -region is a thermal activation energy gap which is strongly dependent on  $H$ .  
© 1996 American Institute of Physics. [S0021-8979(96)58808-7]

The magnetotransport and magnetic properties of the perovskite  $\text{La}_{1-x}\text{A}_x\text{MnO}_{3+\delta}$  ( $0 \leq x \leq 1$ ) system have received a great amount of attention recently after the discovery of the so-called colossal magnetoresistance (CMR) effect in the ferromagnetic phase (FM) of this system.<sup>1–6</sup> Essential to the CMR is the existence of the mixed valence state of Mn, evolving from  $\text{Mn}^{3+}$  (spin  $S=2$ ) in the parent phase ( $x=0$ ) to  $\text{Mn}^{4+}$  (spin  $S=3/2$ ) in the end compound such as  $\text{CaMnO}_3$  (i.e.,  $A=\text{Ca}$ ). The low energy  $t_{2g}^3$  triplet contributes a local spin of  $S=3/2$  to both  $\text{Mn}^{3+}$  and  $\text{Mn}^{4+}$ . In addition,  $\text{Mn}^{3+}$  has an additional electron in the  $e_g^1$  state with its spin parallel to the local spin, whereas the  $e_g^1$  state is empty in  $\text{Mn}^{4+}$ . Whether the  $e_g^1$  electron is localized or mobile depends on the local spin orientation. If the local spins are aligned as in a FM, the  $e_g^1$  electron will be mobile so as to lower its kinetic energy. However in the AFM configuration, the intra-atomic exchange between the  $e_g^1$  electron and the local spin would forbid the electron transfer, hence, resulting in a charge localization. Because of these reasons, the electron transport in  $\text{La}_{1-x}\text{A}_x\text{MnO}_3$  is sensitive to an underlying magnetic structure and its dynamics.<sup>7</sup> It is believed that the origin of CMR is directly related to this sensitivity.

To date, research on CMR has focused on the FM phase, in particular, on  $\text{La}_{0.67}\text{Ca}_{0.33}\text{MnO}_3$  and other similar compounds.<sup>1–4</sup> CMR as large as ten-thousandfold has been obtained in polycrystals,<sup>3</sup> single crystals,<sup>8</sup> and epitaxial thin films.<sup>1,2</sup> A maximum MR is generally associated with the FM phase transition. We have studied the CMR effect using a different approach, and have searched for the maximum MR with an emphasis on the AFM phase. As a consequence we have achieved record CMR values of 830 000% at  $T=125$  K and 10<sup>8</sup>% at  $T=57$  K in a well-prepared  $\text{La}_{0.5}\text{Ca}_{0.5}\text{MnO}_3$  compound. Coupled with such a dramatic CMR is a field induced AFM–FM first order phase transition. At low  $T$ , we have also observed a strongly field dependent activation energy gap in the AFM phase.

The bulk  $\text{La}_{0.5}\text{Ca}_{0.5}\text{MnO}_3$  compound was prepared using

a solid-state reaction method. Appropriate proportions of  $\text{La}_2\text{O}_3$ ,  $\text{CaCO}_3$ , and  $\text{MnO}_2$  precursors were thoroughly mixed and then pressed into pellets. The sintering process lasted over a long period of 150 h in an oxygen atmosphere. Two intermediate grindings and mixings were carried out for homogenization. The annealing temperature was 1200 °C for the first two sinterings and was 1300 °C for the last. The sample was cooled to room temperature in more than 8 h. Four-probe magnetoresistance was measured in a cryostat equipped with an 8 T magnet. The magnetization of the sample was measured using the Quantum Design SQUID magnetometer. X-ray diffraction analysis indicated that the sample has a single phase with a cubic perovskite structure. The lattice constant is 7.66 Å.

Figure 1 shows the temperature ( $T$ ) dependence of resis-

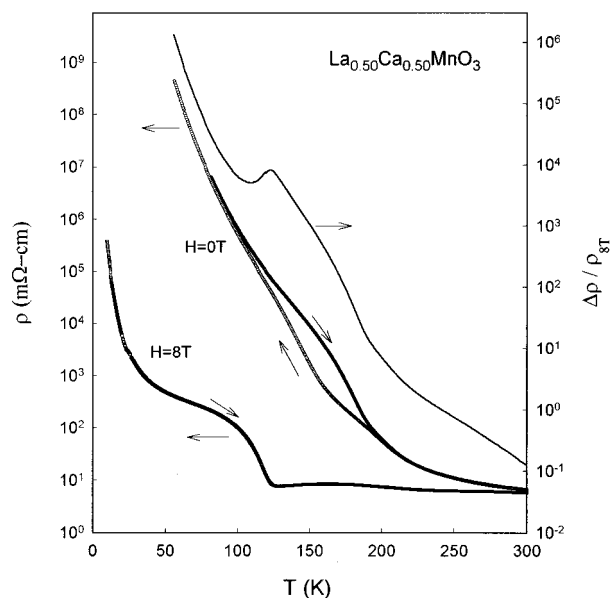


FIG. 1. The temperature ( $T$ ) dependence of the resistivity,  $\rho(T)$ , (in log scale) measured in zero and 8 T field for  $\text{La}_{0.5}\text{Ca}_{0.5}\text{MnO}_3$ . The magnetoresistance ratio defined as  $[\rho_0(T) - \rho_{8T}(T)] / \rho_{8T}(T)$  is also shown. The arrows indicate directions of measurement.

<sup>a)</sup>Electronic mail: gxiao@watson.ibm.edu

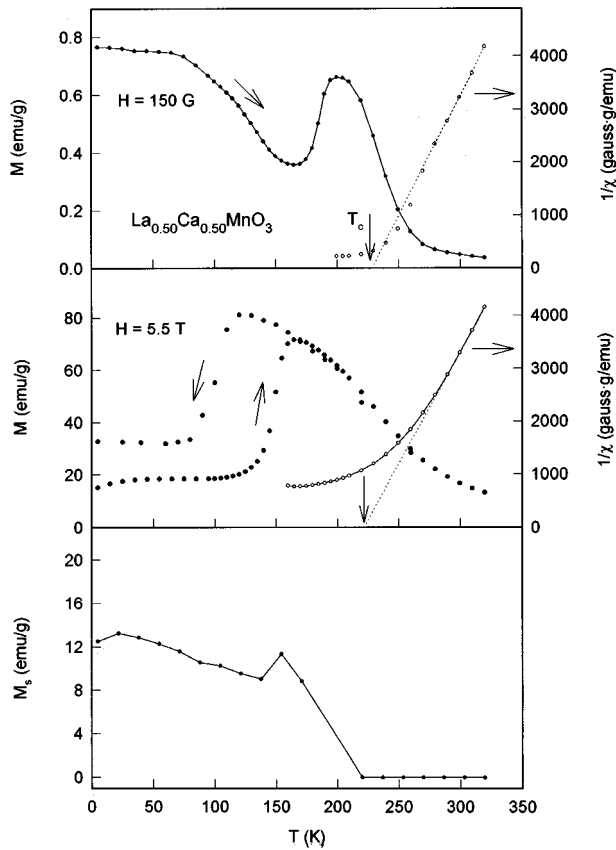


FIG. 2. The  $T$ -dependence of magnetization  $M(T)$  and inverse susceptibility  $\chi^{-1}(T)$  measured at  $H=150$  G and 5.5 T. By extrapolating  $M(H)$  in the high- $H$  region to  $H=0$ , we have obtained a small ferromagnetic spontaneous magnetization  $M_s(T)$  which is shown in the lower panel.

tivity,  $\rho(T)$ , (in log scale) measured in 0 and 8 T field. The zero field  $\rho_0(T)$  reveals a thermal hysteresis between 110 and 190 K in the cooling and warming-up mode. The  $\rho_{8T}(T)$  at 8 T was measured only during warming-up. Over the  $T$ -range studied,  $\rho_0(T)$  experiences a change spanning over eight orders of magnitude. Its  $T$ -dependence is semiconductorlike with an activation energy  $\Delta(0) \approx 67$  meV. On the other hand,  $\rho_{8T}(T)$  is substantially smaller than  $\rho_0(T)$  at any given  $T$ . Above 120 K,  $\rho_{8T}(T)$  is weakly dependent on  $T$ , having a value (a few m $\Omega$ -cm) typical of a poor metal. Below 120 K,  $\rho_{8T}(T)$  experiences a sudden increase and evolves into an activation region with a gap  $\Delta(8T) \approx 7.5$  meV, which is about one order of magnitude smaller than  $\Delta(0)$ . Also shown in Fig. 1 is MR ratio defined as  $[\rho_0(T) - \rho_{8T}(T)]/\rho_{8T}(T)$ . At  $T \approx 60$  K  $\rho$  changes over six orders of magnitude between 0 and 8 T, and at  $T \approx 125$  K over four orders of magnitude. To our knowledge the CMR effect shown here is the largest reported in  $\text{La}_{1-x}\text{A}_x\text{MnO}_3$  and similar systems. It is noted that the maximum CMR in the FM  $\text{La}_{0.67}\text{Ca}_{0.33}\text{MnO}_3$  occurs near  $T_c$  and vanishes as  $T$  approaches zero. However, in  $\text{La}_{0.5}\text{Ca}_{0.5}\text{MnO}_3$ , CMR seems to increase exponentially with reducing  $T$ .

To understand the anomalous magnetotransport, we have measured the magnetic properties of  $\text{La}_{0.5}\text{Ca}_{0.5}\text{MnO}_3$ . Figure 2 shows the  $T$ -dependence of magnetization  $M(T)$  and inverse susceptibility  $\chi^{-1}(T)$  measured in a low field (150 G)

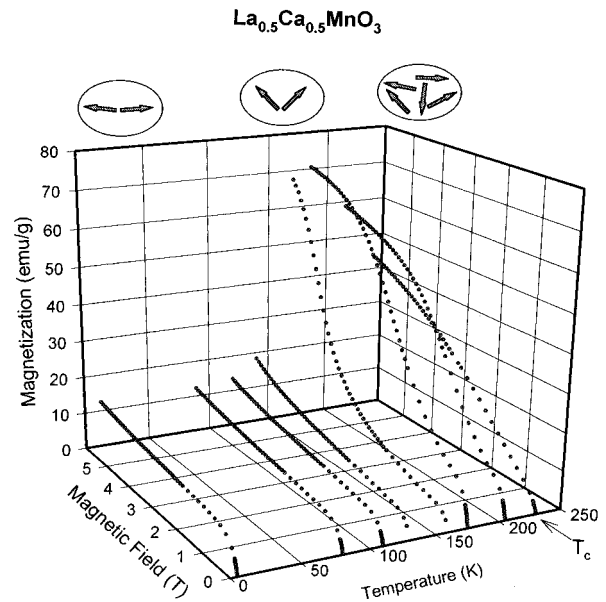


FIG. 3. Magnetization curves  $M(H)$  measured at various temperatures. Three magnetic states are shown schematically in various temperature regions: a canted antiferromagnet, a canted ferromagnet, and a paramagnet.

and a high field (5.5 T). We have also measured a series of  $M(H)$  curves from 0 to 5.5 T and in the  $T$ -range between 5 and 230 K. Some representative  $M(H)$  curves are shown in Fig. 3. By extrapolating  $M(H)$  in the high- $H$  region to  $H=0$ , we have obtained a small FM spontaneous magnetization  $M_s(T)$ , which is shown in the lower panel of Fig. 2. Based on Figs. 2 and 3, we describe some of the important features of the magnetic properties.

(1) There exist two magnetic transitions in the  $T$ -range studied. The high- $T$   $\chi^{-1}(T)$  provides an extrapolated Curie-Weiss  $T_c \approx 225$  K as shown in Fig. 2, indicating a FM transition from a paramagnetic state. Another magnetic transition occurs at a  $T_d$  lower than  $T_c$ . The transition temperature,  $T_d$ , depends on  $H$  and on thermal history (zero-field-cooled or field-cooled). The substantial drop of  $M$  below  $T_d$  is indicative of an FM-AFM transition. The thermal hysteresis in  $M$  vs  $T$  (see the middle panel of Fig. 2) reveals a first order phase transition.

(2) At a fixed  $T$ , the FM-AFM transition can also be induced by an applied  $H_d$  (see Fig. 3). At a low  $T$  ( $< 100$  K), the solid is an AFM up to the maximum 5.5 T of our instrument. At a high  $T$ , for example, 150 K, the AFM-FM transition starts at about 4 T. As  $T$  approaches  $T_c$ , the AFM-FM transition shifts to a lower  $H$ , and becomes much smeared. In the zero  $H$  field, the solid is probably never a FM even at  $T$  near  $T_c$ . For example, at  $T=205$  K, the  $M(H)$  curve is hardly of any FM nature.

(3) Under a high  $H$  (e.g., 5.5 T),  $M$  approaches  $\sim 90$  emu/g as  $T \rightarrow 0$  K. Comparing with the theoretical limit of  $M_0 = 102$  emu/g, one concludes that the canting angle  $\theta_{\text{FM}}$  is about  $56^\circ$  at  $H=5.5$  T in the FM phase [note that  $\cos(\theta/2) = M_s^{\text{exp}}/M_0$ .] On the other hand, in the AFM phase, the spin orientations are canted too as evidenced from a small FM  $M_s(T)$  component shown in the lower panel of Fig. 2. We

estimated that  $\theta_{\text{AFM}} \approx 165^\circ$ . In other words, the AFM–FM transition, that can be either induced by  $H$  or by varying  $T$ , corresponds to a transition in  $\theta$  from  $165^\circ$  to  $56^\circ$ .

With the above magnetic properties in mind, we can proceed to explain the magnetotransport data presented in Fig. 1. In zero field,  $\theta$  remains large between 5 K and  $T_c$ . As a consequence, a charge transfer between neighboring sites is difficult, according to the prediction of the double exchange model<sup>9–11</sup> that charge transfer integral  $t$  is proportional to  $\cos(\theta/2)$ . At low  $T$ , charges are almost fully localized, which leads a thermally activated  $\rho_0(T)$ . Neutron diffraction studies<sup>12</sup> on  $\text{Pr}_{0.5}\text{Sr}_{0.5}\text{MnO}_3$  have shown that  $\text{Mn}^{3+}$  and  $\text{Mn}^{2+}$  sites are spatially ordered at a low  $T$  similar to a Wigner lattice.

At a high  $H$  (e.g., 8 T), the system is FM above  $T \approx 125$  K. In the FM phase, because of a much smaller canting angle, the charge transfer is enhanced substantially, allowing the formation of extended electronic states. The solid then behaves like a metal, albeit a poor one, with a resistivity of a few  $\text{m}\Omega\text{-cm}$ . At about 125 K, a FM–AFM transition occurs, causing a charge localization and a thermally activated transport. However, as mentioned earlier, the energy gap at 8 T is much smaller than that at zero field. This is due to the fact that the canting angle in the AFM phase is reduced in the high  $H$  region because of the Zeeman energy. A smaller canting angle makes the charge transfer easier. In short, the dramatic CMR effect in the low- $T$  region observed in Fig. 1 is caused by the strongly  $H$  dependent energy gap  $\Delta(H)$  in the AFM phase. This differs from the CMR mechanism in the FM  $\text{La}_{0.67}\text{Ca}_{0.33}\text{MnO}_3$ , where the effect of  $H$  is to suppress the randomness in spin orientation. The dynamics of the two phenomena, though related, is very different.

Recently Tomioka *et al.*,<sup>5</sup> have studied a single crystal of  $\text{Pr}_{0.5}\text{Sr}_{0.5}\text{MnO}_3$  which shows similar magnetic and transport properties to those presented here. The CMR effect they reported, however, is much smaller. Application of a field of 7 T changes  $\rho$  by about two orders of magnitude at  $T \approx 0$  K.

Comparing with the  $\text{La}_{0.5}\text{Ca}_{0.5}\text{MnO}_3$  system that has a MR of one-millionfold, the latter seems to develop a much more rigid charge-ordered lattice, yielding a larger energy gap in the AFM phase. The metallic phases of the two systems, on the other hand, do share a similar resistivity (a few  $\text{m}\Omega\text{-cm}$ ).

In summary, we have obtained record values of CMR in the AFM phase of  $\text{La}_{0.5}\text{Ca}_{0.5}\text{MnO}_3$ . At  $T = 125$  K, the CMR is about one million percent. It increases exponentially to 100 million percent at 57 K. The CMR effect at intermediate  $T$ 's (e.g., 125 K) is associated with a field induced first order FM–AFM phase transition. In the low- $T$  region ( $< 100$  K), the AFM phase leads to a charge localization and, possibly, spatially charge ordering. The energy gap in the insulating AFM phase is dependent on  $H$ , with a higher  $H$  corresponding to a smaller gap. It is this particular nature of the energy gap in the AFM phase that brings about the phenomenal CMR effect.

This work was supported in part at Brown University by NSF under the Materials Research Group Grant No. DMR-9121747, and partially by DMR-9414160.

- <sup>1</sup>R. von Helmolt, J. Wecker, B. Holzapfel, L. Schultz, and K. Samwer, *Phys. Rev. Lett.* **71**, 2331 (1993).
- <sup>2</sup>S. Jin, T. H. Tiefel, M. McCormack, R. A. Fastnacht, R. Ramesh, and L. H. Chen, *Science* **264**, 413 (1994).
- <sup>3</sup>S. Jin, H. M. O'Bryan, T. H. Tiefel, M. McCormack, and W. W. Phodes, *Appl. Phys. Lett.* **66**, 382 (1995).
- <sup>4</sup>M. F. Hundley, M. Hawley, R. H. Heffner, Q. X. Jia, J. J. Neumeier, J. Tesmer, J. D. Thompson, and X. D. Wu, *Appl. Phys. Lett.* **67**, 860 (1995).
- <sup>5</sup>Y. Tomioka, A. Asamitsu, Y. Moritomo, H. Kuwahara, and Y. Tokura, *Phys. Rev. Lett.* **74**, 5108 (1995).
- <sup>6</sup>G. Q. Gong, C. L. Canedy, Gang Xiao, J. Z. Sun, A. Gupta, and W. J. Gallagher, *Appl. Phys. Lett.* (in press).
- <sup>7</sup>J. Inoue and S. Maekawa, *Phys. Rev. Lett.* **74**, 3407 (1995).
- <sup>8</sup>A. Urushibara, Y. Moritomo, T. Arima, A. Asamitsu, G. Kido, and Y. Tokura, *Phys. Rev. B* **51**, 14 103 (1995).
- <sup>9</sup>P.-G. de Gennes, *Phys. Rev.* **118**, 141 (1960).
- <sup>10</sup>C. Zener, *Phys. Rev.* **82**, 403 (1951).
- <sup>11</sup>P. W. Anderson and H. Hasegawa, *Phys. Rev.* **100**, 675 (1955).
- <sup>12</sup>K. Knížek, Z. Jiráček, E. Pollert, F. Zounová, and S. Vratislav, *J. Solid State Chem.* **100**, 292 (1992).